Spark-discharge Plasma as a Method to Produce Low AC Loss Multifilamentary (RE)$Ba_2Cu_3O_7$ Coated Conductors

Tom B. Mitchell-Williams, Algirdas Baskys, Yina Guo, Simon C. Hopkins, Ursel Bangert, Alexander Molodyk, Valery Petrykin, Fedor Gömöry, Lubomir Frolek and Bartek A. Glowacki

***Abstract*— If coated conductors are to be used in large-scale AC applications such as motors and generators, energy losses must be minimised. Hysteretic AC losses can be reduced by dividing the coated conductor into filaments. In this work a new method for producing filamentary coated conductors is presented. An electrical spark discharge was used to selectively degrade regions of superconducting tape. The robust, non-contact and scalable method was used to striate tapes into 4 filaments. The filamentary samples had lower AC losses than non-striated tapes with less than a 7% reduction in current carrying capacity.**

***Index Terms*— AC losses, Coated conductors, High-temperature superconductors, Materials processing.**

I. Introduction

The problem of AC losses in high temperature superconductors (HTS) in the form of coated conductors (CC's) complicates their use in large scale applications. In addition to the energy loss the increased cryogenic load on the system can negate the improved efficiency that superconducting cables provide. The extreme aspect ratio of the HTS layer in CC's is the source of the high hysteretic loss, particularly when the external field is perpendicular to the face of the CC tape. It has been demonstrated that dividing the tape into *n* narrower filaments can reduce the hysteretic loss by a factor of *n* [1]–[3]. Additionally, coupling losses, due to resistive current flow between filaments, can be reduced by increasing the resistive barriers between superconducting regions and ensuring their transposition [4], [5].

Previous methods including mechanical scribing [6], [7], laser striation [8]–[10], inkjet printing [11]–[13] and substrate templating [14], [15] have been used to divide CC's into filaments. In the current work an alternative method using high temperature plasma, which occurs during an electrical spark-discharge between electrode and tape surface, is presented. This new method is scalable, non-contact, low-cost and can be adapted to adjust the level of degradation induced during the striation procedure.

II. Experimental Methods

A. Superconducting tape

The 12 mm wide tape from SuperOx used had a nominal minimum I_c rating of 430 A at self-field and 77 K. The basic architecture of the tape is similar to that produced by several manufacturers. The tape is based on a 60 µm thick Hastelloy substrate, with the functional layers deposited by the IBAD-MgO/PLD-GdBCO route. The stabilizer consisted of a 2 µm silver layer, giving a total tape thickness of approximately 65 µm. Some samples had the Ag cap layer removed chemically using a 1:1:2 solution of H_2O_2:NH_3(aq):H_2O. The silver free samples were used to compare if there was an advantage to striating without the Ag cap layer in terms of the resulting width of the striated region.

B. Spark discharge control

Spark-discharges were produced during the dielectric breakdown of air between electrodes held at high voltage. The voltage was generated using a voltage multiplier circuit (VMC). This converted 4.2 V DC input voltage to a maximum of ~20 kV output across the electrodes, with ~450 V output used in practice. The input voltage and current were controlled using a regulated DC power supply (Kenwood PD 18-30). The lateral precision of the spark-discharge was improved by using a needle (radius of curvature 0.15 mm) as one of the electrodes. The motion of the tape with respect to the electrodes was controlled using a 3-axis mechanical stage (custom *xyz* stage, Soul Kozak). A schematic of the set-up is shown in Fig. 1. The electrode-tape distance, relative speed and VMC input power were varied. Tests were performed with and without the silver stabilizer present. Spark-discharging was performed in ambient conditions at atmospheric pressure.

This work was supported in part by the Engineering and Physical Sciences Reasearch Council, U.K. T. B. M-W and A. B would also like to acknowledge financial support from the Worshipful Company of Armourers and Braziers'.

Additional data related to this publication are available at the University of Cambridge data repository (http://dx.doi.org/10.17863/CAM.1670).

T. B. Mitchell-Williams, A. Baskys, and S. C. Hopkins are with the Department of Materials Science and Metallurgy, University of Cambridge, Cambridge, CB3 0FS, U.K. (e-mail: tbm23@cam.ac.uk).

Y. Guo is with the Materials & Surface Science Institute, University of Limerick, Ireland. U. Bangert is with the Department of Physics and Energy, University of Limerick, Ireland.

A. Molodyk is with SuperOx, Moscow, Russia. V. Petrykin is with SuperOx Japan LLC, Tokyo, Japan.

L. Frolek and F. Gömöry are with the Institute of Electrical Engineering, Slovak Academy of Sciences, Slovakia.

B. A. Glowacki is with the Department of Materials Science and Metallurgy, University of Cambridge, Cambridge, CB3 0FS, U.K. and with the Institute of Power Engineering, 02-981 Warsaw, Poland.

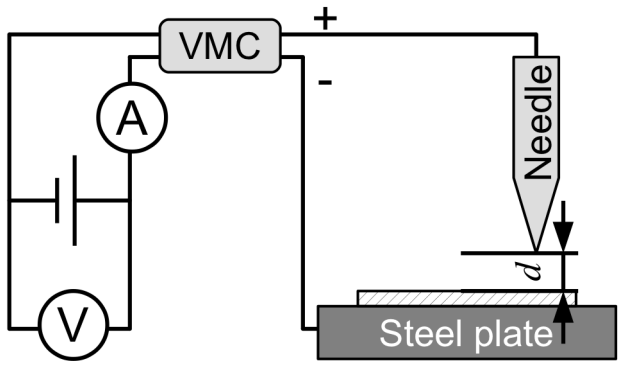

Fig. 1. Schematic diagram of spark-discharge set up. The superconducting tape is represented by the hatched box. The steel plate was electrically isolated from ground. The details of the voltage multiplier circuit (VMC) are not included for simplicity. Not to scale.

C. Hall probe magnetometry

Samples 24 mm long were zero-field cooled to 77 K in liquid nitrogen and magnetized using an electromagnet with an applied field of 140 mT. The trapped magnetic field was measured by a Hall probe (HHP-VA, Arepoc) as it was scanned above the sample surface using a bespoke 3-axis stage controlled by in-house software. Measurements were started 300 s after magnetization to avoid any significant effects due to flux creep. The scan height was 0.5 mm and lateral step size 0.25 mm.

D. Critical current measurement

The critical currents of silver stabilized samples 40 mm in length were measured before and after striation. Samples were tested at 77 K in liquid nitrogen and zero external magnetic field. Current was supplied (Hewlett Packard 6680A DC power supply) whilst the voltage was measured using a Keithley 182 nanovoltmeter. The current was ramped linearly at a rate of 8 A s^{-1}. Current contacts were 10 mm long at both ends of the sample. Voltage taps were soldered to the silver stabilizer of the tape surface and a criterion of 1 μV cm^{-1} was used to determine I_c. The entire system was controlled using software developed in-house.

E. Microscopy

Scanning electron microscopy (SEM) was performed using two different electron microscopes. For high resolution microanalysis a Hitachi SU-70 SEM with Schottky electron gun was used with a working distance of 15 mm and accelerating voltage of 15 kV. Energy dispersive X-ray spectroscopy (EDX) data were collected using INCA software (Oxford Instruments). Morphology was assessed using secondary electron imaging (JSM-5500LV SEM, JEOL) with a working distance of 10 mm and accelerating voltage of 10 kV.

F. AC loss characterization

The AC losses of 120 mm long samples were measured in an applied AC magnetic field by an established calibration free method [16]. Measurements were performed at 77 K with a field frequency of 72 Hz up to a maximum field of 100 mT(rms). The results were compared with calculations for full-width and multi-filamentary samples using the Brandt-Indenbom model for a superconducting strip in perpendicular AC field [1].

G. Interfilament resistance

Resistance measurements were performed using the 4-point method to determine the resistive barrier between filaments at 77 K. Current was supplied by a 1030 MicroCal Current Source (RS components) and measured using a Keithley 2000 multimeter. Voltage was measured using a Keithley 182 nanovoltmeter. Current was varied between -100 mA and +100 mA in 5 mA steps. Samples were 10 mm long and any silver at the sample edges was removed.

III. Results and Discussion

A. Parameter selection

Single striations were made across the width of several 24 × 12 mm tape pieces and the trapped field profiles measured to determine the parameters required to separate the superconducting regions. The needle height (*d* in Fig. 1), relative linear speed and VMC input power were all varied. It was found that smaller distances, lower speeds and higher input power gave better separated filaments. Small distances, faster speeds and lower power gave narrower striations. Parameters were sought to achieve separated filaments with the minimum reduction in current carrying capacity.

The samples, all with 4 filaments, presented in the current work were all produced using a height, *d*, of 0.15 mm and VMC input power of 2 W. The frequency of discharge was ~20 Hz. The linear velocity of the needle for each of the 4 sample types presented are shown in Table I. Specific samples referred to below have prefixes ‘M’ for magnetic measurements, ‘I’ for critical current and ‘AC’ for AC loss.

The large number of combinations available were not exhausted. Furthermore, other variables such as thickness of stabilizer, atmosphere composition and pressure, needle tip radius and multiple passes were not adjusted either, meaning there is still room for optimization.

TABLE I
PARAMETERS OF THE SAMPLE TYPES

Sample type	Silver present?	Linear velocity / mm s^{-1}	Number of filaments
AgP01	Yes	0.5	4
AgP02	Yes	1.0	4
R01	No	1.0	4
R02	No	2.0	4

B. Trapped field profiles

The trapped field profiles for the 4 sample types are shown in Fig. 2. Samples without silver stabilizer trap slightly lower fields than those with. This can be attributed to the slight damage caused by the etchant to the GdBCO surface during silver removal. All 4 samples showed 4 clear filaments visible, however, in sample M_R02 an indication of filament coupling can be seen between the right and center-right filaments in Fig. 2(d). The electrical connection between these filaments was confirmed by interfilament resistance measurements.

These were the only filaments that were incompletely separated.

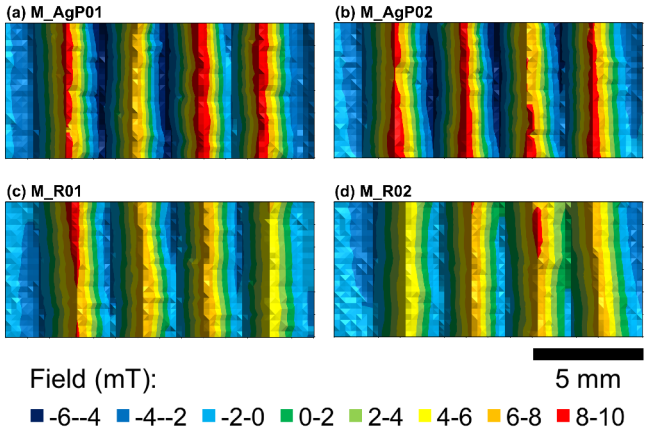

Fig. 2. Contour plots showing the trapped field profiles for the 4 sample types. Samples were zero-field cooled to 77 K. The measurement height was 0.5 mm. Separated filaments can be seen in all samples, however the degree of separation is variable: M_R02 shows signs of slight filament coupling between the right and centre right filaments.

C. *Single discharge impact morphology*

The surface of the HTS layer following a single spark discharge impact is shown in Fig. 3. There are 2 distinct regions within the impact zone. The EDX element maps, Fig. 3(d) and (e), indicate that the central part is exposed Hastelloy whilst the surrounding area is severely degraded GdBCO. The GdBCO region appears to have melted then solidified during the sparking process, microcracks and pores are visible in Fig. 3(b). The rapid melting and solidifying will ensure the damaged GdBCO does not carry a supercurrent and acts as a resistive bridge between the superconducting filaments. This was confirmed by interfilament resistance measurements.

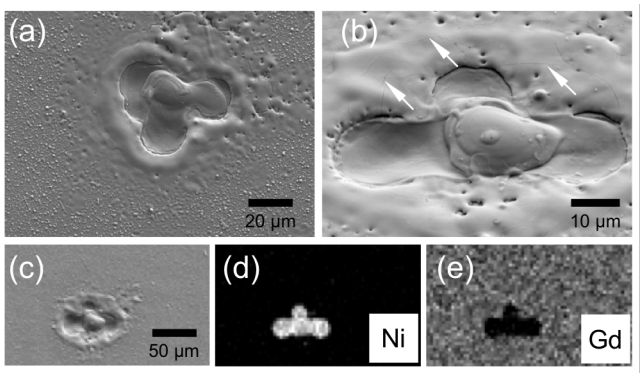

Fig. 3. Tape surface of an un-stabilized sample after a single spark-discharge. (a) SEI at 0° tilt showing damaged region, (b) higher magnification SEI at 45° tilt. The white arrows highlight microcracks in the degraded GdBCO. (c) SEI and (d), (e) corresponding EDX element maps showing the distribution of Ni, a significant component in the Hastelloy substrate, and Gd a component of the HTS layer.

D. *Striation morphology*

The color changes adjacent to the striations, Fig. 4, are due to partial oxidation of the surface due to the temperature of the spark plasma. The actual width of the damaged region is much narrower as is confirmed by SEM imaging, Fig. 5, and I_c measurements, Table II.

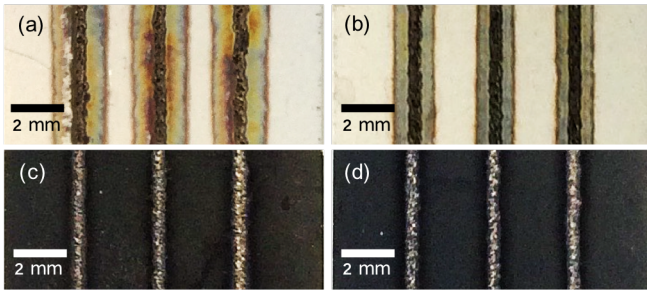

Fig. 4. Photographs of the 4 sample types (a) AgP01, (b) AgP02, (c) R01, (d) R02. The striation width appears superficially larger than the damaged region due to color changes from oxidation occurring during the high temperature spark-discharge.

Differences between the striations can be seen in Fig. 5. The higher density of spark-discharges present in M_AgP01 and M_R01 lead to more exposed Hastelloy regions and consequently a wider striation width than in M_AgP02 and M_R02 respectively.

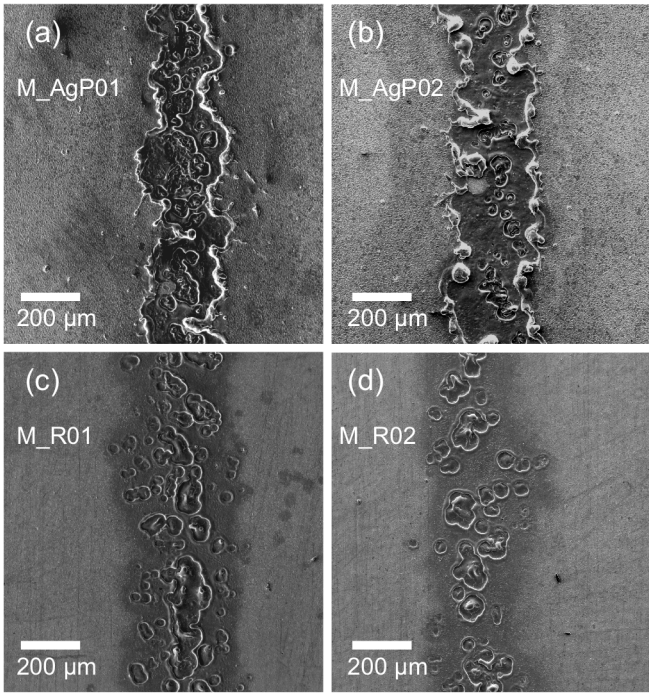

Fig. 5. SEM micrographs (SEI) of the 4 sample types. The centers of the individual spark-discharge regions have not fully coalesced. The silver has been removed by the sparking process from the striated regions in the stabilised samples.

The width of the striations appears similar for M_AgP01 and M_AgP02, however, the greater density of the exposed Hastelloy regions and proximity to the remaining silver in M_AgP01 implies that the damaged GdBCO areas extend further. This is strengthened by the observation of a larger discolored region visible in Fig. 4.

E. *Critical current values*

The critical currents of the silver stabilized samples are given in Table II. The effective width of the striations calculated from the reduction in current carrying capacity are 280 µm and 140 µm for I_AgP01 and I_AgP02 respectively. This is

consistent with the SEM images in Fig 5(a) and (b) and suggests that the damaged HTS layer is slightly wider than apparent striation width for AgP01 and slightly narrower for AgP02. This means that the spark-discharge process can produce striations that do not significantly damage the HTS layer beyond the impact region.

TABLE II
CRITICAL CURRENTS

Sample	I_c before striation / A	I_c after striation / A	Reduction in I_c / %
I_AgP01	443	413	6.8
I_AgP02	456	440	3.5

F. *Interfilament resistance*

The average interfilament resistance for the 4 sample types is given in Table III. Using the equivalent resistor model used in [4], [5], [8] and a resistivity of Hastelloy at 77 K of 1.24 μΩ.m [17] the barrier resistance, R_b, was calculated. The barrier resistance was much greater than the Hastelloy, suggesting good separation, which should prevent significant coupling losses. The barrier resistance was higher for the samples without the silver cap layer because no redeposition of Ag could occur to provide a lower resistance path. The samples striated using a lower linear velocity, and consequently a higher number of discharges per unit length, had a higher barrier resistance due to more extensively damaged interfilament material.

TABLE III
INTERFILAMENT RESISTANCE

Sample	Average interfilament resistance per meter / Ω.m	Calculated barrier resistance per meter / Ω.m
M_AgP01	0.80	0.40
M_AgP02	0.46	0.23
M_R01	1.76	0.88
M_R02	1.05	0.52

G. *AC losses*

The AC loss characteristics for each of the sample types are shown in Fig. 6. All 4 have similar behavior across the field range measured. The results are compared with the well verified Brandt-Indenbom model for a superconducting strip [1], using a full width of 12 mm and I_c of 450 A, equation (1).

$$Q = 4\mu_0 a^2 J_{cs} H_a \left(\frac{2J_{cs}}{\pi H_a}\right) \ln\left[\cosh\left(\frac{\pi H_a}{J_{cs}}\right)\right] - \tanh\left(\frac{\pi H_a}{J_{cs}}\right) \quad (1)$$

Where Q is the energy loss per unit length per cycle, μ_0 is the permeability of free space, a is the half width of the superconductor and J_{cs} is the critical sheet current density ($= I_c/2a$).

The samples all have a similar dependence with increasing applied field, with an approximate 2-fold reduction in AC loss at 100 mT, relative to the monolithic case. The most likely cause of the AC loss reduction being lower than the expected 4× is some filament coupling due to incomplete striation of the HTS layer along the entire length of the samples. This contrasts with the interfilament resistance measurements for short samples indicating fully separated filaments.

The filamentary samples and reference sample showed higher measured loss than the Brandt model predicts for field magnitudes below ~20 mT(rms) and ~10 mT(rms) respectively. This is likely to have two main contributions: J_c non-uniformities across the tape width [18], [19] or, in the case of the filamentary samples, magnetic coupling of filaments [20].

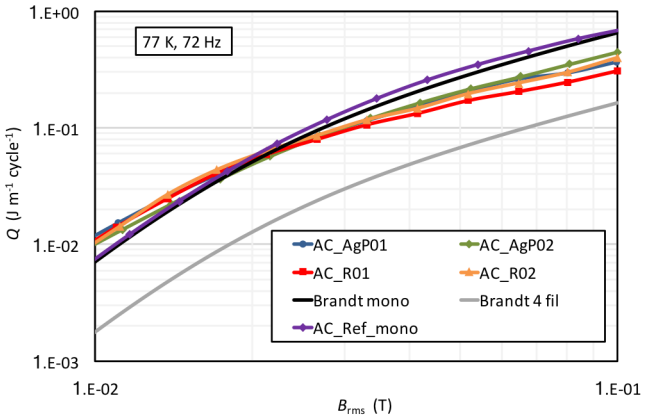

Fig. 6. The magnetization AC loss vs. AC external magnetic field (rms) for all 4 sample types and comparison with a reference monolithic sample and results from the Brandt-Indenbom model. The samples show a reduction in the AC loss for higher applied fields of ~2 times, approximately half the expected 4-fold reduction. Samples measured at 77 K and 72 Hz.

IV. SUMMARY

Spark-discharge plasma striation was shown to be an effective method for producing filamentary coated conductors with reduced AC losses. Spark gap size, power and linear speed were varied to determine parameters that produced well separated filaments. The electrical separation of filaments on short samples was confirmed by Hall probe magnetometry and 4-point resistance measurements. SEM imaging and microanalysis illustrated the morphology of the striations on both silver stabilized and un-stabilized samples. Furthermore, critical current measurements showed that there was negligible degradation beyond the visible striated region.

Samples with 4 filaments were produced. The best sample had a striation width of 140 μm and filaments 2.9 mm wide. The average interfilament resistance per meter, for the same sample, over a short length was 0.46 Ω.m. The effective reduction in I_c following striation was just 3.5% and the AC loss was ~2× lower.

Future work will investigate the effect of multiple passes, electrode tip size and alternative atmospheres on the striation morphology. Also, frequency dependence of the AC loss will be measured.

REFERENCES

[1] E. H. Brandt and M. Indenbom, "Type-II-superconducting strip with current in a perpendicular magnetic field," *Phys. Rev. B*, vol. 48, no. 17, pp. 12894–12906, 1993.

[2] F. Grilli and A. Kario, "How filaments can reduce AC losses in HTS coated conductors," *Supercond. Sci. Technol.*, vol. 29, no. 8, p. 83002, 2016.

[3] E. Zeldov, J. R. Clem, M. McElfresh, and M. Darwin, "Magnetization and transport currents in thin superconducting films," *Phys. Rev. B*, vol. 49, no. 14, pp. 9802–9822, 1994.

[4] E. Demencik, F. Grilli, A. Kario, R. Nast, A. Jung, M. Vojenciak, J. Scheiter, and W. Goldacker, "AC magnetization loss and transverse

resistivity of striated YBCO coated conductors," *IEEE Trans. Appl. Supercond.*, vol. 25, no. 3, pp. 3–7, 2015.

[5] R. Gyuraki, A. Godfrin, A. Jung, A. Kario, R. Nast, E. Demencik, F. Grilli, and W. Goldacker, "Inter-filament Resistance at 77 K in Striated HTS Coated Conductors," *arXiv*, no. Preprint, 2016.

[6] I. Kesgin, G. Majkic, and V. Selvamanickam, "Fully filamentized HTS coated conductor via striation and selective electroplating," *Phys. C Supercond. its Appl.*, vol. 486, pp. 43–50, 2013.

[7] S. P. Ashworth and F. Grilli, "A strategy for the reduction of ac losses in YBCO coated conductors," *Supercond. Sci. Technol.*, vol. 19, no. 2, pp. 227–232, 2006.

[8] N. Amemiya, S. Kasai, K. Yoda, Z. Jiang, G. A. Levin, P. N. Barnes, and C. E. Oberly, "AC loss reduction of YBCO coated conductors by multifilamentary structure," *Supercond. Sci. Technol.*, vol. 17, no. 12, pp. 1464–1471, Dec. 2004.

[9] R. Nast, M. Vojenčiak, E. Demencik, A. Kario, B. Ringsdorf, A. Jung, B. Runtsch, F. Grilli, and W. Goldacker, "Influence of laser striations on the properties of coated conductors," *J. Phys. Conf. Ser.*, vol. 507, no. 2, p. 22023, 2014.

[10] T. Machi, K. Nakao, T. Kato, T. THirayama, and K. Tanabe, "Reliable fabrication process for long-length multi-filamentary coated conductors by a laser scribing method for reduction of AC loss," *Supercond. Sci. Technol.*, vol. 26, p. 105016 (15pp), 2013.

[11] S. C. Hopkins, T. B. Mitchell-Williams, D. R. Vanden Bussche, A. Calleja, V. R. Vlad, M. Vilardell, X. Granados, T. Puig, X. Obradors, A. Usoskin, M. Soloviov, M. Vojenciak, F. Gomory, I. V. Driessche, M. Backer, and B. A. Glowacki, "Low AC Loss Inkjet-Printed Multifilamentary YBCO Coated Conductors," *IEEE Trans. Appl. Supercond.*, vol. 26, no. 3, 2016.

[12] X. Cai, I. Kesgin, R. Schmidt, Y. Chen, V. Selvamanickam, and A. A. Design, "Completely Etch-free Fabrication of Multifilamentary Coated Conductor Using Inkjet Printing and Electrodeposition," *IEEE Trans. Appl. Supercond.*, no. c, pp. 1–5, 2013.

[13] R. C. Duckworth, M. P. Paranthaman, M. S. Bhuiyan, F. A. List, and M. J. Gouge, "AC Losses in YBCO Coated Conductor With Inkjet Filaments," *IEEE Trans. Appl. Supercond.*, vol. 17, no. 2, pp. 3159–3162, 2007.

[14] G. Majkic, I. Kesgin, Y. Zhang, Y. Qiao, R. Schmidt, and V. Selvamanickam, "AC Loss Filamentization of 2G HTS Tapes by Buffer Stack Removal," *IEEE Trans. Appl. Supercond.*, vol. 21, no. 3, pp. 3297–3300, 2011.

[15] A. C. Wulff, M. Solovyov, F. Gömöry, A. B. Abrahamsen, O. V Mishin, A. Usoskin, A. Rutt, J. H. Lundeman, K. Thydén, J. B. Hansen, and J.-C. Grivel, "Two level undercut-profile substrate for filamentary YBa 2 Cu 3 O 7 coated conductors," *Supercond. Sci. Technol.*, vol. 28, no. 7, p. 72001, 2015.

[16] J. Šouc, F. Gömöry, and M. Vojenčiak, "Calibration free method for measurement of the AC magnetization loss," *Supercond. Sci. Technol.*, vol. 18, no. 5, pp. 592–595, 2005.

[17] J. Lu, E. S. Choi, and H. D. Zhou, "Physical properties of Hastelloy C-276 at cryogenic temperatures," *J. Appl. Phys.*, vol. 103, no. 6, p. 64908, 2008.

[18] M. Solovyov, E. Pardo, J. Šouc, F. Gömöry, M. Skarba, P. Konopka, M. Pekarčíková, and J. Janovec, "Non-uniformity of coated conductor tapes," *Supercond. Sci. Technol.*, vol. 26, no. 11, p. 115013, 2013.

[19] F. Grilli, R. Brambilla, and L. Martini, "Modeling high-temperature superconducting tapes by means of edge finite elements," *IEEE Trans. Appl. Supercond.*, vol. 17, no. 2, pp. 3155–3158, 2007.

[20] M. Marchevsky, E. Zhang, Y. Xie, V. Selvamanickam, and P. G. Ganesan, "AC Losses and magnetic coupling in multifilamentary 2G HTS conductors and tape arrays," *IEEE Trans. Appl. Supercond.*, vol. 19, no. 3, pp. 3094–3097, 2009.